

Article

Rapid Fabrication of Pineapple Leaf Fibers from Discarded Leaves by Using Electrolysis of Brine

Huy N. Q. Phan ¹, Jyh Hoang Leu ^{2,*}, Khanh Thien Tran ³, Vi N. D. Nguyen ⁴ and Trung Tan Nguyen ⁵¹ Department of Materials Science and Engineering, Feng Chia University, Taichung 40744, Taiwan² Master's Program of Green Energy Science and Technology, Feng Chia University, Taichung 40744, Taiwan³ Chemical Engineering in Advanced Materials and Renewable Energy Research Group, Van Lang University, Ho Chi Minh 72311, Vietnam⁴ Department of Chemical Engineering, Feng Chia University, Taichung 40744, Taiwan⁵ Office of Academic Affairs, Nha Trang University, Nha Trang 57100, Vietnam

* Correspondence: hjleu@fcu.edu.tw

Abstract: Instead of contributing to global warming by the traditional method—burning crop wastes—in this study, discarded pineapple leaves were rapidly turned into multifunctional fibers: pineapple leaf fibers (PALF). In addition, the presence of pure hydrogen during treatment can be a competitive advantage. PALF were extracted by a conventional technique, then immersed into sodium hydroxide 6% before it was treated with an electrolysis system of sodium chloride 3%. The crystallinity index increased 57.4% of treated PALF, and was collected from XRD. Meanwhile, the removal of hemicellulose and lignin in the fiber formation was presented at the absorbance peak of around 1730 cm⁻¹ by FTIR spectrums. Simultaneously, the purity of hydrogen reached 99% and was confirmed by GC analysis. The obtained PALF and hydrogen can be used for further consideration, aiming for a circular economy.

Keywords: PALF; pineapple leaf treatment; pure hydrogen; electrolysis of brine; agro-waste handling



Citation: Phan, H.N.Q.; Leu, J.H.; Tran, K.T.; Nguyen, V.N.D.; Nguyen, T.T. Rapid Fabrication of Pineapple Leaf Fibers from Discarded Leaves by Using Electrolysis of Brine. *Textiles* **2023**, *3*, 1–10. <https://doi.org/10.3390/textiles3010001>

Academic Editors: Hafeezullah Memon and Narcisa Vrinceanu

Received: 14 November 2022

Revised: 14 December 2022

Accepted: 21 December 2022

Published: 23 December 2022



Copyright: © 2022 by the authors. Licensee MDPI, Basel, Switzerland. This article is an open access article distributed under the terms and conditions of the Creative Commons Attribution (CC BY) license (<https://creativecommons.org/licenses/by/4.0/>).

1. Introduction

Pineapple is the favored and the third most consumed fruit in the world. In 2017, the worldwide area for growing pineapple was 1.1 million hectares, equivalent to 1318 thousand ton parts of leaves released as agro-wastes [1]. Most discarded leaves will be burned and fermented to provide organic fertilizer, as in the conventional method [2]. However, enormous particulate matter (PM) with high concentration has appeared from burning that may cause cardiovascular diseases to humans exposed to it [3]. Furthermore, a significant amount of carbon dioxide (CO₂) released from the pyrolysis of organic compounds will certainly contribute to the dire state of global warming. This affects to net-zero carbon emission target between 2040 and 2060 [4].

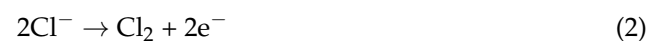
Recently, pineapple leaf has become a candidate to develop into a natural fiber since it contains up to 80–81% cellulose, just 4.6–12% lignin and 6–19% hemicellulose [5]. There are several functions that pineapple leaf fiber (PALF) can take responsibility for, such as heavy metal adsorbent [6], green acoustic absorber [7], thermal insulation material [8], and biodegradable plastic [9].

In the fabrication of PALF, the extraction is a mechanical treatment that was a conventional procedure. This process removed the epidermal tissue of the pineapple leaf to form PALF [10]. There were several kinds of extraction, such as manual extraction, machinery extraction, and the retting process. Adad et al. [11] were successful in using a ceramic plate to extract fiber bundles by applying friction force, but this method is only suitable for the long leaves and requires human effort. Meanwhile, Das et al. [12] revealed the effectiveness of using a machine to extract fibers; it can produce at least 15 kg of fiber per day. However, the operation of this process and the reduction of damage to fiber products

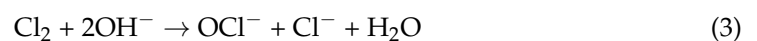
might be considered. According to Asim et al. [13], in the retting process, pineapple leaf was immersed in a solution that contained diammonium phosphate or urea to release the fibers. This method requires a long treatment time and is also a non-eco process. Although those processes can certainly collect PALF, its properties may not satisfy expectations. Hence, chemical treatment, including the softening and bleaching process, was applied as a method to enhance the quality of PALF. The objective here was to remove hemicellulose, lignin, and other substances [14]. In the softening process, sodium hydroxide usage was widely spread [15]. To decolorize and eliminate excess hemicellulose and lignin, the bleaching process with oxidation agents (e.g., hydrogen peroxide, sodium hypochlorite) was an encouraging aid [16,17]. In addition, this chemical treatment also assists to improve the crystallinity and surface morphology of PALF [18]. Gadzama et al. [19] conducted a study that treated PALF with 2% NaOH and 10% NaOCl in 3.25 h can form a fiber in the diameter range of 25–58 nm. Likewise, Cordeiro et al. [20] also reported that surface properties of PALF can be enhanced by treating raw leaves with 4% NaOH and some other chemicals within a couple of hours.

Despite traditional mechanical and chemical methods being dominant in the treatment of pineapple leaves, the application of electrochemical methods to PALF formation seems to be a good alternative; it not only shortens the treatment time, but also reduces CO₂ emission and generates pure hydrogen.

The electrolysis of brine with conditions of no separator and low concentration was mentioned as the procedure to produce high oxidized ions (OCl[−]) [21]. Moreover, a massive amount of pure hydrogen continuously released at the surface of negative electrode [22]. These processes would happen after electrochemical and chemical reactions. Firstly, the reduction of water (Equation (1)) and the oxidation of chloride (Equation (2)) take place on the cathode and the anode surface, respectively:



In the second stage, the hypochlorite formation process begins:



Overall reaction:



In this work, the utilization of a brine electrolysis system for handling pineapple leaves was investigated. Afterwards, the PALF would be analyzed for surface morphology with scanning electron microscopy (SEM), crystallinity index (CI) with X-ray diffraction (XRD), and functional groups with Fourier transform infrared (FTIR) analyzer. Additionally, through gas chromatography (GC) analysis, the presence of hydrogen from electrolysis process also was noticed.

2. Materials and Methods

2.1. The Formation of PALF

The pineapple leaves used collected from a pineapple (*Ananas comosus*) plant in Taiwan (R. O. C.), which is located in East Asia. Similar to the principle of machinery extraction [23], a wooden hammer was used to extract the microfibrils below the leaf epidermis to form PALF. For softening process, the extracted leaves were immersed in sodium hydroxide (NaOH, was purchased from Union Chemical Works Ltd., Hsinchu, Taiwan) which was prepared by stirring 24 g of pellets in 376 g of water to obtain 400 g solution for a concentration of 6%. After 1 h, the softened PALF was moved to the electrolysis system for bleaching with 3% sodium chloride solution (NaCl, was purchased from Union Chemical Works Ltd., Hsinchu, Taiwan) which was acquired from 12 g of particles dissolved in water to 400 g and Pt coated Ti electrodes, and the operating condition 10 V–1.1 A was provided

by DC regulated power supply (TES 6210, Taipei, Taiwan) in 3 h (illustrated in Figure 1). The chemicals used in this work were certified reagent grade. Finally, PALF was dried in a dryer oven (Deng Yng DO45, New Taipei, Taiwan) at 80 °C for 4 h and next ready to analyze the characterizations.

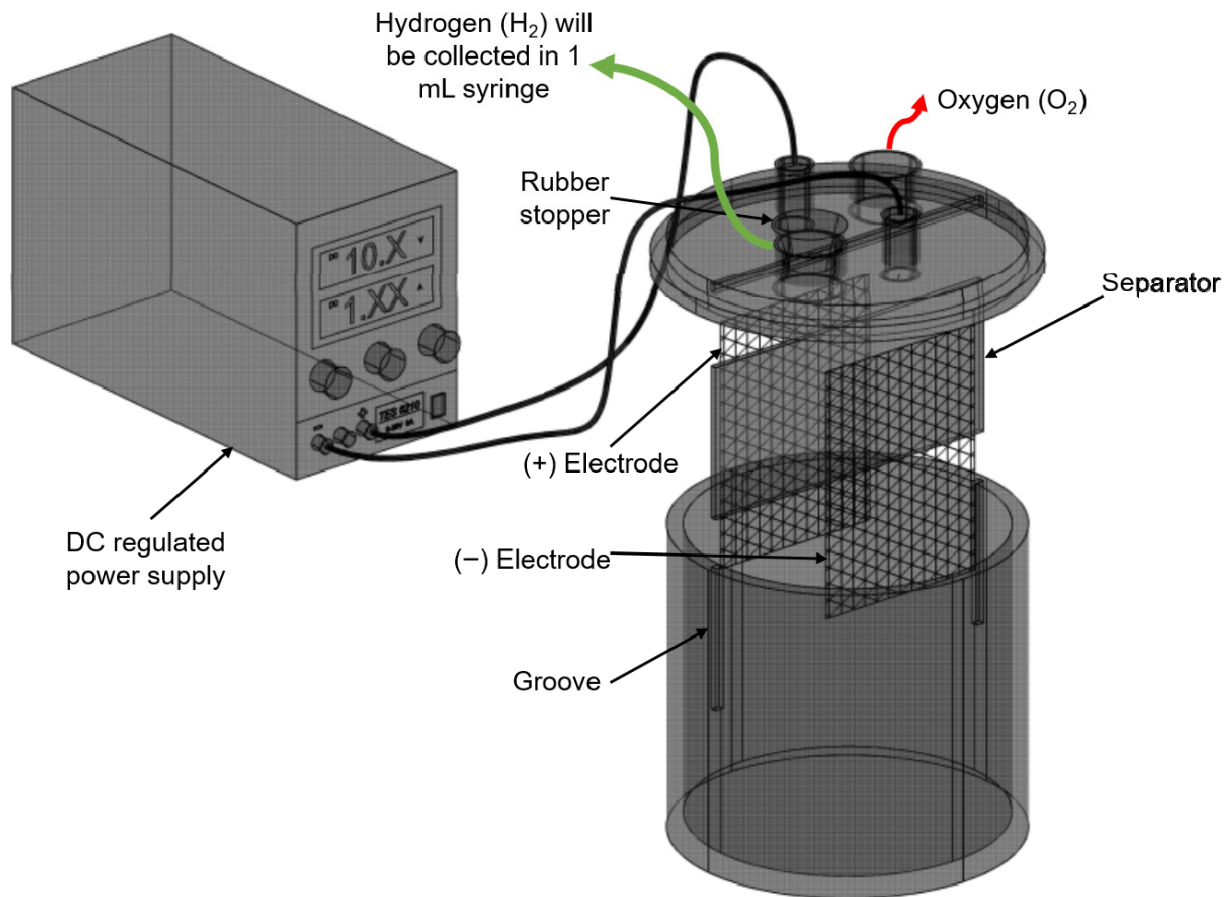


Figure 1. Illustration of electrolysis system with hydrogen collection for GC analyzer by 1 mL syringe.

2.2. Characterization of PALF

The specimen of three different stages was characterized as named untreated-PALF (U-PALF), softened-PALF (S-PALF), and bleached-PALF (B-PALF). The analyzed samples must be dried.

2.2.1. Scanning Electron Microscopy and Visual Appearance

SEM is a necessary analysis that helps to determine the basics of surface morphology and structural changes. The morphological study was performed by SEM machine (Hitachi S4800, Fukuoka, Japan). This instrument was operated with an emitted current of 10,600 nA, accelerated voltage of 3 kV, and working distance between the aperture and specimen was adjusted from 9.2 to 10.4 mm. In addition, the apparent color change visually also verifies the transformation on the fibers structure.

2.2.2. X-ray Diffraction

X-ray diffraction patterns of PALF were collected by using an X-ray diffractometer (Bruker D2 phaser, Billerica, MA, USA) with the operating conditions of voltage and current at 30 kV and 10 mA, respectively. The value of crystallinity index of untreated, softened, and bleached PALF samples were calculated using the method (Equation (5)) proposed by [24].

$$C = \frac{I_{200} - I_a}{I_{200}} \times 100\% \quad (5)$$

where I_{200} corresponds the maximum intensity of diffractogram (at about 22° of 2θ), I_a gives the intensity of amorphous band appeared as the valley between 110 and 200 at 18° of 2θ [25,26]. Furthermore, the crystallite sizes of the PALF samples were determined by Debye-Scherrer's law in Equation (6):

$$D = \frac{K\lambda}{\beta \cos \theta} \quad (6)$$

With D represents the crystallite size (CS), λ is the wavelength of the Cu-K radiation of 0.154 nm, β is Full-Width-Half-Maximum (FWHM) (radians), K is the correction factor of 0.94, and θ (radians) is collected as the diffraction Bragg's angle of the highest peak from XRD diffractogram.

2.2.3. Fourier Transform Infrared Spectroscopy

All dried samples were characterized by using an FTIR spectrometer (PerkinElmer, France). Attached ATR spectroscopy was used to determine the change of functional groups in PALF before and after each treatment step. The spectrums were graphed with wavelengths from 4000 to 650 cm^{-1} .

2.3. Gas Chromatography

To guarantee hydrogen's presence during the period of electrolysis, an gas chromatography (8700 T) has a thermal conductivity detector with carrier gas (argon), stainless-steel pipe column (with a dimension of $1/8 \text{ mm ID} \times 4 \text{ m}$), detector (at 40°C), injector (40°C), column (at 28°C). All hydrogen samples would be collected by taking the gas output from a rubber stopper with 1 mL laboratory syringe.

3. Results and Discussion

3.1. Hypochlorite Production

In the past decade, hypochlorite (OCl^-) was known as a potent oxidizing agent that can react with biological molecules [27]. Thus, it plays a crucial role in oxidizing pineapple leaves to PALF in this study. According to Mohamed et al. [28], immersing PALF into containing OCl^- solution can also reinforce PALF properties. Electrochemical with the presence of chloride can release OCl^- , Equations (1)–(4) have performed that. The amount of hypochlorite can be determined by Faraday's law equation [29]:

$$m = \frac{MIt}{nF} \quad (7)$$

where m is the production of OCl^- (g), M and n are molar mass of OCl^- (g mol^{-1}) and electrons exchanged ($n = 2$), respectively, I is applied current (A), and F represents Faraday constant ($96,487 \text{ C mol}^{-1}$) in time t (h). As such, the total amount of hypochlorite was 3.17 g in 3 h of treatment. The experimental volume was set at 400 mL, the hypochlorite rate per volume (mg L^{-1}) thus was 7919. Similarly, Saleem, et al. [30] showed the electrochemical method can apply to the onsite production of sodium hypochlorite, and the optimal concentration of NaOCl in the study was around $>7000 \text{ mg L}^{-1}$ in 3 h. This result revealed that hypochlorite can be produced greatly by electrolyzing chloride-containing solution. In such manner, the amount of produced hypochlorite with the experimental condition is sufficient to improve PALF in this study.

3.2. Surface Morphology

Based on Figure 2, visual observation showed a difference in the intensity of color and brightness after each treatment step. Plus, cellulose fibers in Figure 2c with an off-white ensured that the oxidation and decolorization occurred during the electrolysis of brine.



Figure 2. Visual images of (a) U-PALF, (b) S-PALF, (c) B-PALF after oven-dried in 4 h at 80 °C.

The SEM analysis results in Figure 3 display the average diameter size of a fiber bundle fluctuated from 30 to 50 μm . It is similar to the Josephine pineapple cultivar, which is known as a species supply the finest fiber bundle with a diameter below 0.1 mm [28]. The surface of untreated fiber bundle presented several defects such as roughness and irregular significantly due to the existence of hemicellulose, lignin, and other impurities. Figure 3b revealed that a part of hemicellulose, lignin, and other substances was removed, and a few single cellulose fibers with a diameter of 3.8 to 5 μm also were observed. Afterwards, Figure 3c exhibited absolutely improvement in morphology. The surface of PALF became smoother with a neat arrangement along with the apparent formation of cellulose fibers after softening and bleaching treatment. In general, electrolysis bleaching was an akin performance compared to Fareez, et al. [31], who conducted PALF formation with NaOH and pure NaOCl instead of NaOH and NaOCl from the electrolysis of weak brine.

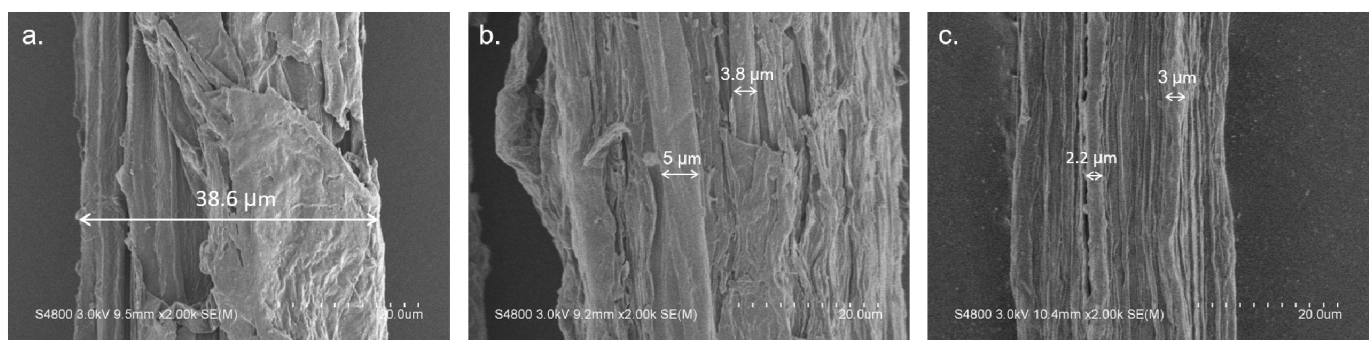


Figure 3. SEM images of a fiber bundle with (a) U-PALF, (b) S-PALF, (c) B-PALF.

3.3. Crystallinity Index

The objective of XRD analysis was to realize the crystallinity proceeding of cellulose fibers. The crystallization characteristics and XRD patterns of untreated, softened, and bleached PALF were shown in Figure 4. It presents three peaks of Bragg diffraction angle (denoted by 2θ) from 15.39° to 15.54°, 16.45° to 16.65°, and 22.2° to 22.35° for reflection assigned to 1–10, 110, and the 200 crystallographic planes, respectively. This result accurately indicated the presence of cellulose I crystal as demonstrated by French [32]. Additionally, the crystalline phase of cellulose was an essential factor that decides the properties of natural fibers [33]. Hence, these peaks have increased conspicuously after each stage of the treatment was a positive result in applying electrochemical for handling discarded pineapple leaves.

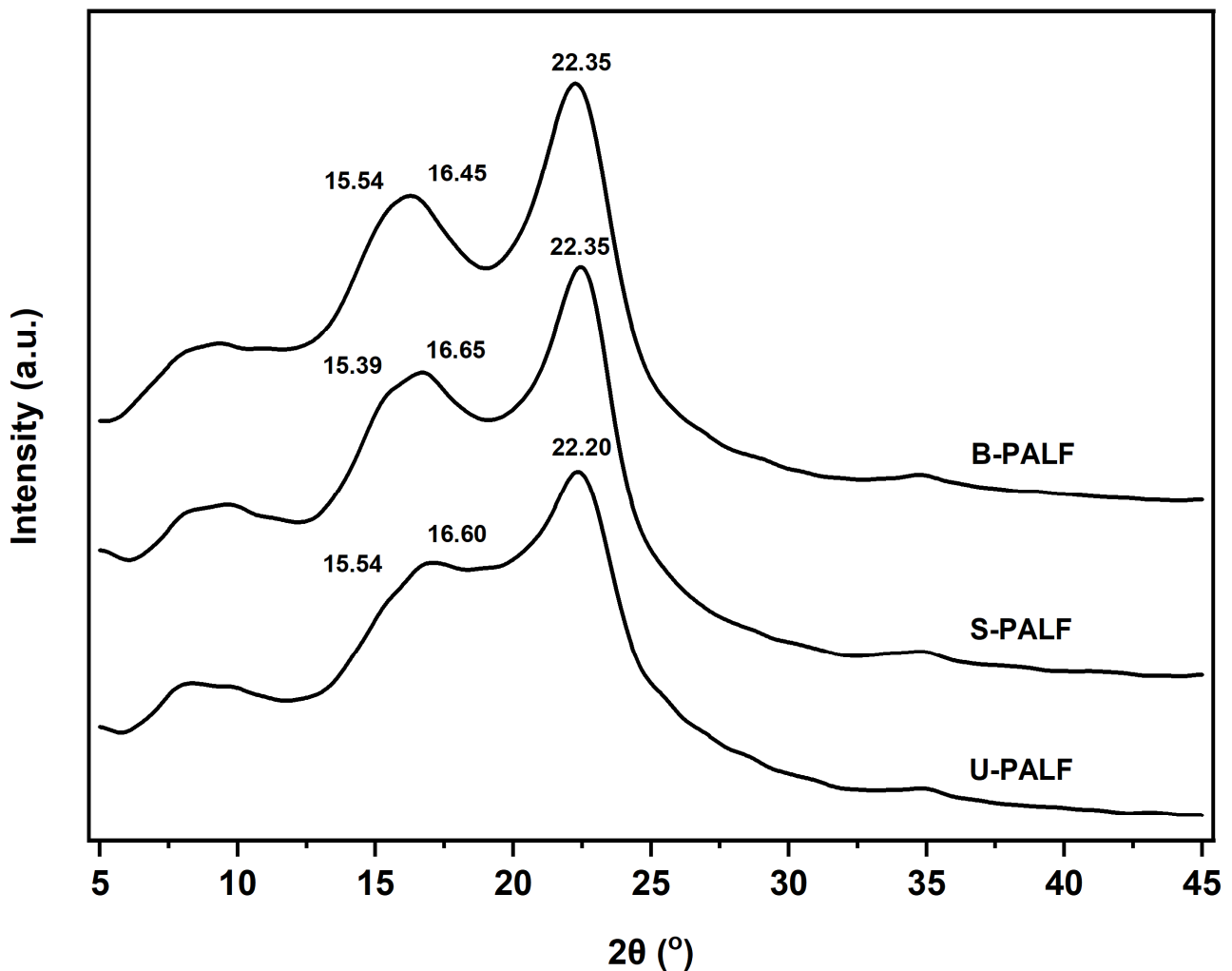


Figure 4. XRD pattern of PALF with untreated, softened, and bleached sample.

Based on Segal's equation, the crystallinity index of bleached cellulose was affirmed higher than untreated cellulose, approximately 57.4%. The index of each stage has shown in Table 1. In fact, the CI of cellulose may differ on the source and extraction procedure [34,35]. The crystallinity increased after softening and bleaching cellulose fibers has been revealed in several studies. The CI of isolated cellulose from pineapple leave was treated with sodium hydroxide, sodium hypochlorite, and acetic acid was higher than the untreated one [31]. After being treated with sodium hydroxide, acetic acid, and sodium chloride, coconut fiber showed the CI of cellulose was greater than a usual fiber [36]. According to Mtibe et al. [37] and Rambabu et al. [38], the crystallinity increase is due to the realignment of cellulose molecules in the crystal lattice. It will occur during the hemicellulose and lignin removal process in amorphous regions.

Table 1. Crystallinity index and crystallite size of PALF.

PALF	Crystallinity Index (%)	Crystallite Size (nm)
Untreated	28.12	2.28
Softened	36.9	2.56
Bleached	44.26	2.49

The crystallite size of bleached cellulose had a diameter of 2.5 nm was larger than 2.2 nm of the untreated cellulose, which was calculated by using the Debye-Scherrer equation. Line broadening of Full-Half-at-Width-Maximum value is inversely proportional

to the crystallite size value [39]. Therefore, the crystallite size of bleached cellulose was decreased which compared to softened cellulose might be due to local conditions during the electrolysis process, it caused the degree of line broadening relative highly.

3.4. Functional Groups

FTIR was commonly used to determine the difference of functional groups in fiber chemical composition after and before treatment. The spectrums of untreated, softened, and bleached PALF were shown in Figure 5. All the strong and broad transmittance bands were located at around the region of 3340, 2920, 1733, 1635, 1425, 1243, 1160, 1102, and 1032 cm^{-1} . These wavelength positions may vary slightly depending on the analyzed PALF samples. The location at around 3340 cm^{-1} has revealed the hydrogen bond of the O–H functional group [14] which was identified as the represented group for the main chemical properties of cellulose matrix. In addition, the reduction in transmittance intensity of O–H vibration stretching after each treatment stage indicated the participation of free hydroxyl groups existed in chemical reactions [40].

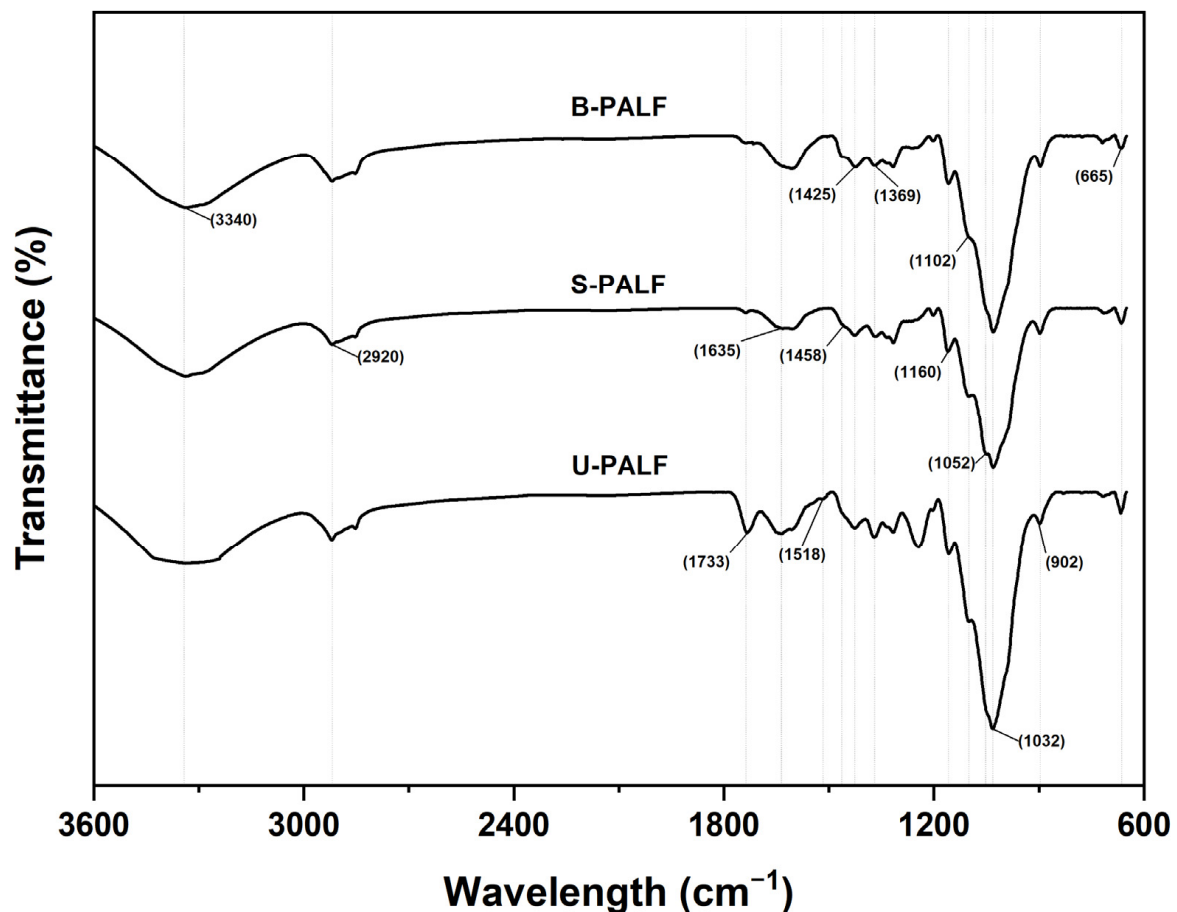


Figure 5. FTIR spectrums of PALF with untreated, softened, and bleached sample.

Furthermore, a narrow band at valley 2920 cm^{-1} proved the presence of C–H stretching from methyl groups ($-\text{CH}_3$) of hemicellulose and cellulose [41]. The amount of this group has tended to decrease gradually in this study. The protrusion of absorbance peaks at 1733, 1518, and 1243 cm^{-1} indicated the $-\text{C}=\text{O}$ group of lignin and hemicellulose, the $-\text{C}=\text{C}-$ group of lignin, and the $-\text{COO}$ group of hemicellulose, respectively. In general, the rearrangement of amorphous cellulose and the removal of lignin, hemicellulose, and other impurities during processing were the validation for this agreement [31]. Oven-drying was a key point in preventing the water molecules interacting with the cellulose fibers. Thus, there was no appearance of water molecules at band 1635 and 1640 cm^{-1}

in S-PALF and B-PALF, respectively, which was found. According to Lee et al. [42], the observed vibrational bands from around 1450 to 1400 cm^{-1} (at 1458 and 1425 cm^{-1} in this study) were due to the existence of CH_2 symmetrical bending. Besides, the bending of CH was supposed to form the absorbance peak at band 1369 cm^{-1} . The region from 1260 to 1350 cm^{-1} had a few scattered absorption peaks as an effect of C–O stretching vibration [42]. Corresponding to the research has been revealed by Fareez et al. [31], the presence of small peaks at wavenumber 1160, 1102, 1052, 1032, and 902 cm^{-1} presented for the stretching of C–O–C, stretching of C–O at C–3, stretching of C–O at C–6, stretching of C–O–C, and bending of C–CH, respectively. Lastly, the attribution of monoclinic phases cellulose was attributed to the band at around 665 cm^{-1} wavelength [43].

3.5. The Presence of Hydrogen

GC is a common type of chromatography applied to separate and analyze the percentage of hydrogen in a gas mixture. The presence of hydrogen during the whole electrolysis process has been shown in Table 2. Numerous hydrogen was produced continuously within the first couple of minutes when electrochemical started. Simultaneously, the purity of hydrogen was reached approximately 99% at this time. Therefore, this technique has been considered the most suitable for hydrogen production without the emission of pollution [44]. Moreover, continuity is also crucial in generating pure hydrogen during pineapple leaf treatment. According to Tennakone [22], hydrogen has been released continuously at the negative electrode (cathode) in the electrolysis of brine. Thus, its percentage has remained stable and fluctuated at around 99% throughout the reaction time. On the other hand, oxygen was also known as a basic gas of water electrolysis. However, with the presence of chloride, the chlorine-produced reaction has been more dominant than the oxygen-produced reaction. It can be explained that the standard electrode potential of chlorine (1.35 V) is larger than standard electrode potential of oxygen (1.23 V) [45]. Therefore, oxygen was produced insignificantly in this study. There are still some deficiencies in analyzing released gases, therefore more investigations should be conducted for further consideration in another study.

Table 2. Percent composition of hydrogen in a mixture of 1 mL of gas.

Gas	Percentage in 1 mL of Gas (%)			
	15 min	1 h	2 h	3 h
Hydrogen (H_2)	98.68 ± 0.15	99.23 ± 0.23	99.15 ± 0.18	99.28 ± 0.21
Others (N_2 , CO_2)	1.31 ± 0.15	0.77 ± 0.23	0.85 ± 0.18	0.72 ± 0.21

4. Conclusions

This study demonstrated the successful use of the electrolysis of brine in pineapple discarded leaves treatment. A significant improvement in the morphology and color of PALF, with a diameter of 3.8 to 5 μm and smoother and neater on surface, was indicated by visual and SEM images. Based on XRD diffractograms, the CI of the final treated samples was higher 57.4% than the raw one; crystallite size also changed after each stage. Meanwhile, the removal of hemicellulose and lignin was confirmed by FTIR spectrum, at bands of 1733 cm^{-1} , the absorption peaks have decreased conspicuously. Lastly, GC analysis presented the hydrogen gas with 99% purity.

Author Contributions: J.H.L. and H.N.Q.P. conceptualization; J.H.L. and H.N.Q.P. methodology; J.H.L. validation; H.N.Q.P. investigation; H.N.Q.P. and V.N.D.N. data curation; H.N.Q.P., K.T.T. and T.T.N. writing—original draft preparation; H.N.Q.P., K.T.T. and T.T.N. writing—review and editing; H.N.Q.P. and V.N.D.N. visualization; J.H.L. supervision. All authors have read and agreed to the published version of the manuscript.

Funding: This work was financed by the Ministry of Science and Technology, Taiwan (MOST 110-2926-I-035-001-MY4).

Institutional Review Board Statement: Not applicable.

Informed Consent Statement: Not applicable.

Data Availability Statement: The data presented in this study are available on request from the corresponding author.

Acknowledgments: We gratefully acknowledge the devoted support for analytical instruments and laboratory from the Department of Materials Science and Engineering, Green Energy Development Center and Precision Instrument Support Center, Feng Chia University, Taichung, Taiwan.

Conflicts of Interest: The authors declare no conflict of interest.

References

1. Pandit, P.; Pandey, R.; Singha, K.; Shrivastava, S.; Gupta, V.; Jose, S. Pineapple Leaf Fibre: Cultivation and Production. In *Pineapple Leaf Fibers: Processing, Properties and Applications*; Jawaid, M., Asim, M., Tahir, P.M., Nasir, M., Eds.; Springer: Singapore, 2020; pp. 1–20. [\[CrossRef\]](#)
2. Todkar, S.S.; Patil, S.A. Review on mechanical properties evaluation of pineapple leaf fibre (PALF) reinforced polymer composites. *Compos. Part B Eng.* **2019**, *174*, 106927. [\[CrossRef\]](#)
3. Ferreira, L.E.; Muniz, B.V.; Bittar, T.O.; Berto, L.A.; Figueroba, S.R.; Groppo, F.C.; Pereira, A.C. Effect of particles of ashes produced from sugarcane burning on the respiratory system of rats. *Environ. Res.* **2014**, *135*, 304–310. [\[CrossRef\]](#) [\[PubMed\]](#)
4. Gabrielli, P.; Gazzani, M.; Mazzotti, M. The Role of Carbon Capture and Utilization, Carbon Capture and Storage, and Biomass to Enable a Net-Zero-CO₂ Emissions Chemical Industry. *Ind. Eng. Chem. Res.* **2020**, *59*, 7033–7045. [\[CrossRef\]](#)
5. Mwaikambo, L. Review of the history, properties and application of plant fibres. *Afr. J. Sci. Technol.* **2006**, *7*, 120–133.
6. Daochalermwong, A.; Chanka, N.; Songsrirote, K.; Dittanet, P.; Niamnuy, C.; Seubsai, A. Removal of Heavy Metal Ions Using Modified Celluloses Prepared from Pineapple Leaf Fiber. *ACS Omega* **2020**, *5*, 5285–5296. [\[CrossRef\]](#)
7. Putra, A.; Prasetyo, I.; Selamat, Z. Green Acoustic Absorber from Pineapple Leaf Fibers. In *Pineapple Leaf Fibers: Processing, Properties and Applications*; Jawaid, M., Asim, M., Tahir, P.M., Nasir, M., Eds.; Springer: Singapore, 2020; pp. 143–165. [\[CrossRef\]](#)
8. Rajeshkumar, G.; Ramakrishnan, S.; Pugalenti, T.; Ravikumar, P. Performance of Surface Modified Pineapple Leaf Fiber and Its Applications. In *Pineapple Leaf Fibers: Processing, Properties and Applications*; Jawaid, M., Asim, M., Tahir, P.M., Nasir, M., Eds.; Springer: Singapore, 2020; pp. 309–321. [\[CrossRef\]](#)
9. Ramli, S.; Sheikh Md Fadzullah, S.; Mustafa, Z. The effect of alkaline treatment and fiber length on pineapple leaf fiber reinforced poly lactic acid biocomposites. *J. Teknol.* **2017**, *79*, 111–115. [\[CrossRef\]](#)
10. Jose, S.; Salim, R.; Ammayappan, L. An Overview on Production, Properties, and Value Addition of Pineapple Leaf Fibers (PALF). *J. Nat. Fibers* **2016**, *13*, 362–373. [\[CrossRef\]](#)
11. Adam, A.; Yusof, Y.; Yahya, A. Extraction of pineapple leaf fibre: Josapine and moris. *J. Eng. Appl. Sci.* **2016**, *11*, 161–165.
12. Das, P.; Nag, D.; Debnath, S.; Nayak, L. Machinery for extraction and traditional spinning of plant fibres. *Indian J. Tradit. Knowl.* **2010**, *9*, 2.
13. Asim, M.; Abdan, K.; Jawaid, M.; Nasir, M.; Dashtizadeh, Z.; Ishak, M.R.; Hoque, M.E. A Review on Pineapple Leaves Fibre and Its Composites. *Int. J. Polym. Sci.* **2015**, *2015*, 950567. [\[CrossRef\]](#)
14. Gaba, E.W.; Asimeng, B.O.; Kaufmann, E.E.; Katu, S.K.; Foster, E.J.; Tiburu, E.K. Mechanical and Structural Characterization of Pineapple Leaf Fiber. *Fibers* **2021**, *9*, 51. [\[CrossRef\]](#)
15. Zin, M.H.; Abdan, K.; Mazlan, N.; Zainudin, E.S.; Liew, K.E. The effects of alkali treatment on the mechanical and chemical properties of pineapple leaf fibres (PALF) and adhesion to epoxy resin. *Iop Conf. Ser. Mater. Sci. Eng.* **2018**, *368*, 012035. [\[CrossRef\]](#)
16. Gedik, G.; Avinc, O. Bleaching of Hemp (*Cannabis Sativa* L.) Fibers with Peracetic Acid for Textiles Industry Purposes. *Fibers Polym.* **2018**, *19*, 82–93. [\[CrossRef\]](#)
17. Khaliq, A.D.; Chafidz, A.; Maddun, F.R.; Herimawan, H.R.; Yusuf, G.M.; Rahmillah, F.I. The use of hydrogen peroxide and sky stabilizer agent in bleaching process of textile fabrics. *Aip Conf. Proc.* **2019**, *2138*, 050011. [\[CrossRef\]](#)
18. Tanpichai, S.; Witayakran, S. All-cellulose composite laminates prepared from pineapple leaf fibers treated with steam explosion and alkaline treatment. *J. Reinf. Plast. Compos.* **2017**, *36*, 1146–1155. [\[CrossRef\]](#)
19. Gadzama, S.W.; Sunmonu, O.K.; Isiaku, U.S.; Danladi, A. Isolation and characterization of nanocellulose from pineapple leaf fibres via chemo-mechanical method. *Sci. World J.* **2020**, *15*, 100–105.
20. Cordeiro, N.; Gouveia, C.; John, M.J. Investigation of surface properties of physico-chemically modified natural fibres using inverse gas chromatography. *Ind. Crop. Prod.* **2011**, *33*, 108–115. [\[CrossRef\]](#)
21. Bommaraju, T.V.; Orosz, P.J.; Sokol, E.A. Brine electrolysis. *Electrochem. Encycl.* **2007**, 1–17.
22. Tennakone, K. Hydrogen from brine electrolysis: A new approach. *Int. J. Hydrog. Energy* **1989**, *14*, 681–682. [\[CrossRef\]](#)
23. Banik, S.; Nag, D.; Debnath, S. Utilization of pineapple leaf agro-waste for extraction of fibre and the residual biomass for vermicomposting. *Indian J. Fibre Text. Res.* **2011**, *36*, 2.
24. Segal, L.; Creely, J.J.; Martin, A.E.; Conrad, C.M. An Empirical Method for Estimating the Degree of Crystallinity of Native Cellulose Using the X-Ray Diffractometer. *Text. Res. J.* **1959**, *29*, 786–794. [\[CrossRef\]](#)

25. French, A.D.; Santiago Cintrón, M. Cellulose polymorphy, crystallite size, and the Segal Crystallinity Index. *Cellulose* **2013**, *20*, 583–588. [[CrossRef](#)]
26. Nam, S.; French, A.D.; Condon, B.D.; Concha, M. Segal crystallinity index revisited by the simulation of X-ray diffraction patterns of cotton cellulose I β and cellulose II. *Carbohydr. Polym.* **2016**, *135*, 1–9. [[CrossRef](#)] [[PubMed](#)]
27. Fukuzaki, S. Mechanisms of Actions of Sodium Hypochlorite in Cleaning and Disinfection Processes. *Biocontrol Sci.* **2006**, *11*, 147–157. [[CrossRef](#)] [[PubMed](#)]
28. Mohamed, A.R.; Sapuan, S.M.; Shahjahan, M.; Khalina, A. Effects of Simple Abrasive Combing and Pretreatments on the Properties of Pineapple Leaf Fibers (Palf) and Palf-Vinyl Ester Composite Adhesion. *Polym.-Plast. Technol. Eng.* **2010**, *49*, 972–978. [[CrossRef](#)]
29. He, T.; Kar, M.; McDaniel, N.D.; Randolph, B.B. Electrochemical Hydrogen Production. In *Springer Handbook of Electrochemical Energy*; Breitkopf, C., Swider-Lyons, K., Eds.; Springer: Berlin/Heidelberg, Germany, 2017; pp. 897–940. [[CrossRef](#)]
30. Saleem, M.; Chakrabarti, B.; Hasan, D.u.; Islam, M.S.; Yussof, R.; Hajimolana, Y.S.; Hussain, M.; Khan, G.M.; Si Ali, B. On site Electrochemical Production of Sodium Hypochlorite Disinfectant for a Power Plant utilizing Seawater. *Int. J. Electrochem. Sci.* **2012**, *7*, 3929–3938.
31. Fareez, I.M.; Ibrahim, N.A.; Wan Yaacob, W.M.H.; Mamat Razali, N.A.; Jasni, A.H.; Abdul Aziz, F. Characteristics of cellulose extracted from Jospine pineapple leaf fibre after alkali treatment followed by extensive bleaching. *Cellulose* **2018**, *25*, 4407–4421. [[CrossRef](#)]
32. French, A.D. Idealized powder diffraction patterns for cellulose polymorphs. *Cellulose* **2014**, *21*, 885–896. [[CrossRef](#)]
33. Komuraiah, A.; Kumar, N.S.; Prasad, B.D. Chemical Composition of Natural Fibers and its Influence on their Mechanical Properties. *Mech. Compos. Mater.* **2014**, *50*, 359–376. [[CrossRef](#)]
34. Masahisa, W. Synchrotron-radiated X-ray and neutron diffraction study of native cellulose. *Cellulose* **1997**, *4*, 221–232. [[CrossRef](#)]
35. Park, S.; Baker, J.O.; Himmel, M.E.; Parilla, P.A.; Johnson, D.K. Cellulose crystallinity index: Measurement techniques and their impact on interpreting cellulase performance. *Biotechnol. Biofuels* **2010**, *3*, 10. [[CrossRef](#)] [[PubMed](#)]
36. Benini, K.C. Chemical modification effect on the mechanical properties of HIPS/ coconut fibers composites. *Bioresources* **2010**, *5*, 1143–1155.
37. Mtibe, A.; Liganiso, L.Z.; Mathew, A.P.; Oksman, K.; John, M.J.; Anandjiwala, R.D. A comparative study on properties of micro and nanopapers produced from cellulose and cellulose nanofibres. *Carbohydr Polym* **2015**, *118*, 1–8. [[CrossRef](#)] [[PubMed](#)]
38. Rambabu, N.; Panthapulakkal, S.; Sain, M.; Dalai, A.K. Production of nanocellulose fibers from pinecone biomass: Evaluation and optimization of chemical and mechanical treatment conditions on mechanical properties of nanocellulose films. *Ind Crop Prod* **2016**, *83*, 746–754. [[CrossRef](#)]
39. Revol, J.; Dietrich, A.; Goring, D. Effect of mercerization on the crystallite size and crystallinity index in cellulose from different sources. *Can. J. Chem.* **2011**, *65*, 1724–1725. [[CrossRef](#)]
40. Samal, R.K.; Ray, M.C. Effect of chemical modifications on FTIR spectra. II. Physicochemical behavior of pineapple leaf fiber (PALF). *J. Appl. Polym. Sci.* **1997**, *64*, 2119–2125. [[CrossRef](#)]
41. Mopoung, S. Microporous Activated Carbon Fiber from Pineapple Leaf Fiber by H₃PO₄ Activation. *Asian J. Sci. Res.* **2016**, *9*, 24–33. [[CrossRef](#)]
42. Lee, C.H.; Khalina, A.; Lee, S.H.; Padzil, F.N.M.; Ainun, Z.M.A. Physical, Morphological, Structural, Thermal and Mechanical Properties of Pineapple Leaf Fibers. In *Pineapple Leaf Fibers: Processing, Properties and Applications*; Jawaid, M., Asim, M., Tahir, P.M., Nasir, M., Eds.; Springer: Singapore, 2020; pp. 91–121. [[CrossRef](#)]
43. Sugiyama, J.; Persson, J.; Chanzy, H. Combined infrared and electron diffraction study of the polymorphism of native celluloses. *Macromolecules* **1991**, *24*, 2461–2466. [[CrossRef](#)]
44. Ojaomo, K.; Erinle, T.; Oladebeye, D.H.; Olakolegan, D. Hydrogen Generation through Electrolysis of Brine for Clean Energy Development in a Depressed Economy. *IARJSET Int. Adv. Res. J. Sci. Eng. Technol.* **2020**, *7*, 94–101. [[CrossRef](#)]
45. Kraft, A.; Stadelmann, M.; Blaschke, M.; Kreysig, D.; Sandt, B.; Schröder, F.; Rennau, J. Electrochemical water disinfection Part I: Hypochlorite production from very dilute chloride solutions. *J. Appl. Electrochem.* **1999**, *29*, 859–866. [[CrossRef](#)]

Disclaimer/Publisher's Note: The statements, opinions and data contained in all publications are solely those of the individual author(s) and contributor(s) and not of MDPI and/or the editor(s). MDPI and/or the editor(s) disclaim responsibility for any injury to people or property resulting from any ideas, methods, instructions or products referred to in the content.